THE JOURNAL OF BIOLOGICAL CHEMISTRY VOL. 286, NO. 45, pp. 39072–39081, November 11, 2011

Core-glycosylated Mucin-like Repeats from MUC1 Are an Apical Targeting Signal*[S]

Received for publication, August 3, 2011, and in revised form, September 18, 2011 Published, JBC Papers in Press, September 20, 2011, DOI 10.1074/jbc.M111.289504

Carol L. Kinlough[‡], Paul A. Poland[‡], Sandra J. Gendler[§], Polly E. Mattila[‡1], Di Mo[‡], Ora A. Weisz[‡], and Rebecca P. Hughey[‡2]

From the [‡]Department of Medicine, Renal-Electrolyte Division, University of Pittsburgh School of Medicine, Pittsburgh, Pennsylvania 15261 and the [§]Department of Biochemistry and Molecular Biology and Tumor Biology Program, Mayo Clinic College of Medicine, Mayo Clinic Scottsdale, Scottsdale, Arizona 85259

Background: MUC1 apical delivery in polarized MDCK cells employs a path used by proteins with glycan-dependent targeting signals.
Results: Core *O*-glycans on mucin-like repeats of MUC1 act as an apical targeting signal.
Conclusion: MUC1 apical targeting is *O*-glycan-dependent.
Significance: We have identified a specific sequence with a post-translational modification that can direct apical delivery of MUC1 or a reporter protein.

MUC1 is efficiently delivered to the apical surface of polarized Madin-Darby canine kidney (MDCK) cells by transit through apical recycling endosomes, a route associated with delivery of apical proteins with glycan-dependent targeting signals. However, a role for glycans in MUC1 sorting has not been established. A key feature of MUC1 is a heavily *O*-glycosylated mucin-like domain with a variable number of nearly perfect tandem repeats and adjacent imperfect repeats. Metabolic labeling, cell surface biotinylation, immobilized lectins, and confocal immunofluorescence microscopy were used to characterize the polarized delivery of MUC1 mutants and chimeras in MDCK cells to identify the apical targeting signal. Both the interleukin-2 receptor α subunit (Tac) and a chimera where the Tac ectodomain replaced that of MUC1 were delivered primarily to the basolateral surface. Attachment of the MUC1 mucin-like domain to the N terminus of Tac enhanced apical but not basolateral delivery when compared with Tac. Conversely, deletions within the mucin-like domain in MUC1 reduced apical but not basolateral delivery when compared with MUC1. In pull-down assays with lectins, we found a notable difference in the presence of core 1 *O*-glycans, but not poly-*N*-acetyllactosamine, in apically targeted MUC1 and chimeras when compared with Tac. Consistent with these data, we found no effect on MUC1 targeting when galectin-3, with preference for poly-*N*-acetyllactosamine, was depleted from polarized MDCK cells. However, we did block the apical targeting activity of the mucin-like repeats when we overexpressed CMP-Neu5Ac:GalNAc-Rα2,6-sialyltransferase-1 to block core *O*-glycan synthesis. The cumulative data indicate that the core-glycosylated mucin-like repeats of MUC1 constitute an apical targeting signal.

MUC1 is a transmembrane glycoprotein that functions in signal transduction through interaction with cytoplasmic proteins and by modifying transcription factor activity after nuclear targeting of its small subunit (for reviews, see Refs. 1 and 2). Because MUC1 is normally restricted to the apical surface of polarized epithelial cells but is aberrantly localized to all cell surfaces or intracellular membranes in tumor cells (3, 4), we are interested in identifying the features of this protein that regulate its membrane trafficking. Our previous studies identified sites in the MUC1 cytoplasmic domain for adaptor protein binding (AP-1, AP-2, and Grb2) and Cys palmitoylation that altogether modulate its relatively slow clathrin-mediated endocytosis and fast recycling from endosomes (5, 6). Glycosylation of the mucin-like ectodomain also affects cell surface expression because we found that modification with shorter *O*-glycans in glycosylation-defective CHO cells slows delivery to the cell surface from the biosynthetic pathway and increases MUC1 internalization (7).

Glycans on transmembrane proteins can act as apical targeting signals as well as enhancing surface delivery from the biosynthetic pathway (for reviews, see Refs. 8 and 9). In line with these studies, we found that MUC1 is efficiently targeted to the apical surface of polarized Madin-Darby canine kidney (MDCK)[3] cells via apical recycling endosomes (AREs), a pathway selectively used for delivery of apical proteins with glycan-dependent targeting signals (10). Galectin-3 (Gal-3) is thought to play a key role in apical targeting of glycoproteins with lipid raft-independent targeting signals by cross-linking cargo in *trans*-Golgi network-derived vesicles, and we recently reported that MUC1 synthesized in MDCK cells preferentially binds to canine Gal-3 (11–13). However, there is no direct proof that MUC1 apical targeting is either galectin- or glycan-dependent.

* This work was supported, in whole or in part, by National Institutes of Health Grants DK54787 (to R. P. H.), DK054407 (to O. A. W.), CA64389 (to S. J. G.) and P30 DK079307 (Pittsburgh Center for Kidney Research Core C). This work was also supported by the Genzyme Renal Innovations Program (to R. P. H.).
[S] The on-line version of this article (available at http://www.jbc.org) contains supplemental Fig. S1.
[1] Supported by individual NRSA F32DK082109.
[2] To whom correspondence should be addressed: Dept. of Medicine, Renal-Electrolyte Division, S933 Scaife Hall, 3550 Terrace St. Pittsburgh, PA 15261. Tel.: 412-383-8949; Fax: 412-383-8956; E-mail: hugheyr@pitt.edu.

[3] The abbreviations used are: MDCK, Madin-Darby canine kidney; ARE, apical recycling endosome; IP, immunoprecipitate; LEA, *L. esculentum* agglutinin (tomato lectin); PNA, peanut agglutinin; polylactosamine, poly-*N*-acetyllactosamine; R, imperfect repeat; ST6GalNAc-1, CMP-Neu5Ac:GalNAc-Rα2,6-sialyltransferase-1; TR, nearly perfect tandem repeat; WGA, wheat germ agglutinin.

A prominent feature of the MUC1 ectodomain is the variable number of mucin-like nearly perfect tandem repeats (TRs) of 20 amino acids with five or six Ser/Thr residues that serve as sites for *O*-linked glycosylation with GalNAc (14). The TRs are flanked by five proximal and two distal imperfect repeats (Rs) with 4–9 Ser/Thr residues each (see Fig. 1*A* for details). In previous studies, both MUC1 with 30 TR and a mutant MUC1 lacking its cytoplasmic tail were localized using confocal immunofluorescence microscopy to the apical surface of MDCK cells growing on coverslips, whereas the lymphocyte-specific model protein CD2 was localized to the basolateral surface of MDCK cells (15). A chimera of the CD2 ectodomain and MUC1 transmembrane and cytoplasmic tail was also present at the basolateral surface, whereas a chimera of the MUC1 ectodomain and CD2 transmembrane and cytoplasmic tail was apical, suggesting that an apical targeting signal is present in the MUC1 ectodomain (see Fig. 1*B*) (15).

In the present study, we used metabolic labeling, cell surface biotinylation, immobilized lectins, and confocal immunofluorescence microscopy to dissect the features of the MUC1 ectodomain that target it to the apical cell surface in polarized MDCK cells growing on permeable supports. Surprisingly, we found no role for Gal-3 or its ligand, poly-*N*-acetyllactosamine (polylactosamine), in apical targeting of MUC1. Rather, core *O*-glycans on mucin-like repeats of MUC1 constitute an apical targeting signal.

EXPERIMENTAL PROCEDURES

Recombinant cDNAs and Adenovirus—The cDNAs for MUC1 with 22 tandem repeats (MUC1–22TR), MUC1 with two tandem repeats (MUC1–2TR), and Tac-MUC1 chimera were prepared and subcloned into pcDNA3(neo) (Invitrogen) as described previously (5, 6, 16). See Fig. 1 for models of all constructs and details on sequences of *nearly perfect* TRs and adjacent *imperfect* repeats (*R*). The cDNA for MUC1–0R-FLAG in pCI(neo) (Promega, Madison, WI) was obtained from Tony Hollingsworth (University of Nebraska Medical Center, Omaha, NE) (17). The cDNA for full-length wild-type Tac (interleukin-2 receptor α-subunit from Michael S. Marks (University of Pennsylvania, Philadelphia, PA)) was subcloned into pcDNA3(neo) to produce a type 1 transmembrane protein of 251 amino acids after cleavage of the 21-residue signal sequence. The signal sequence of Tac was replaced with the N terminus of MUC1, including five proximal R and one distal R, with or without 22 TRs (550 amino acids or 108 amino acids, respectively, plus the MUC1 cleavable signal sequence), to produce the chimera 22TR-Tac or 0TR-Tac, respectively. The cDNA for CMP-Neu5Ac:GalNAc-Rα2,6-sialyltransferase-1 (ST6GalNAc-1) with a C-terminal vesicular stomatitis virus-G epitope tag was obtained from Joyce Taylor-Papadimitriou (Guy's Hospital, London, UK) and subcloned into pcDNA3 (18).

Stably Transfected Cell Lines—MDCK cells were transfected with (i) pcDNA3(neo) encoding either MUC1–22TR, MUC1–2TR, Tac-MUC1, 22TR-Tac, 0TR-Tac, Tac or ST6GalNAc-1 or (ii) pCI(neo) encoding MUC1–0R-FLAG. Clonal cell lines were screened with anti-MUC1 antibody B27.29 (Fujiribio, Malvern, PA), anti-Tac (anti-CD25 from Ancell (Bayport, MN)), or anti-ST6GalNAc-1 (monoclonal 2C3 from Ulla Mandel (19) (University of Copenhagen, Denmark). MDCK cells expressing ST6GalNAc-1 (neo) (named MDCK+ST6) were stably transfected with pcDNA(hygro) encoding Tac and 0TR-Tac. Cells were grown in G418 (0.5 mg/ml) with or without hygromycin (0.4 mg/ml) as indicated and Dulbecco's modified Eagle's medium (DMEM) and Ham's F-12 (1:1) with 5% fetal bovine serum at 37 °C in a humidified incubator with 5% CO_2 (Invitrogen). Clonal cell lines were isolated and screened by SDS-PAGE after metabolic labeling and immunoprecipitation.

Surface Delivery in Polarized MDCK Cells—Polarized cultures of MDCK cells were grown on 12-mm Costar permeable supports (Corning Glass) with 0.4-μm membranes on 12-well plates for 4 days before use. Cell surface delivery was assayed as described previously (6, 7, 10). Briefly, cells were starved for 30 min in medium lacking Met/Cys (Sigma), metabolically labeled for 30 min with [^{35}S]Met/Cys (Easy Tag Express-[^{35}S]Protein Labeling Mixture, PerkinElmer Life Sciences), and chased up to 120 min in normal culture medium. All steps were carried out in a 37 °C incubator with 5% CO_2. Duplicate filters were moved to ice at each time point. After all time points were collected, the cells on duplicate filters were treated with sulfo-NHS-SS-biotin on either the apical or basolateral surface on ice (6, 7, 10). Cell extracts were prepared, and recombinant proteins were recovered by immunoprecipitation with either anti-MUC1 TR mouse monoclonal antibody B27.29 for MUC1, MUC1–2TR, and 22TR-Tac; mouse monoclonal anti-FLAG epitope antibody (Sigma) for MUC1–0R-FLAG; or mouse monoclonal anti-Tac (CD25) antibody (Ancell) for Tac-MUC1, 0TR-Tac, and Tac. Armenian hamster monoclonal anti-MUC1 cytoplasmic tail antibody CT-2 (20) was included for immunoprecipitation of MUC1, MUC1–2TR, and Tac-MUC1. Immunoprecipitates (IP) were washed and eluted by boiling into 60 μl of 1% SDS. An aliquot (25%) was retained to calculate the total IP, and the remaining 75% was diluted 20-fold with a solution of HEPES-buffered 0.5% Triton X-100 and incubated with avidin-conjugated beads to recover biotinylated proteins. Both the total IP and biotinylated proteins were subjected to SDS-PAGE on 4–15% gradient gels before drying and analysis with a Kodak TR screen and a Bio-Rad Personal Imager and Quantity One software. Data are presented as the percentage of the total IP delivered to the cell surface at each time point for multiple experiments (mean ± S.E.).

Binding to Lectins Conjugated to Beads—Polarized MDCK cells expressing MUC1–22TR, 22TR-Tac, 0TR-Tac, or Tac and growing on permeable supports were metabolically labeled with [^{35}S]Met/Cys for 30 min and chased for 90 min as described above. For analysis of lectin binding, immunoprecipitates were prepared as already described and eluted into SDS (an aliquot saved as total IP where indicated), diluted with 1% Triton X-100 in HEPES-buffered saline, and incubated with 50 μl of a 50% slurry of either tomato lectin (*Lycopersicon esculentum*; LEA) or wheat germ agglutinin (*Triticum vulgare*; WGA) conjugated to beads (4–5 mg of lectin protein/ml slurry, EY Laboratories, Inc. (San Mateo, CA)) overnight with end-over-end mixing. Immunoprecipitates were treated with recombinant *Clostridium perfringens* neuraminidase (New England Biolabs, Ipswich, MA) or reaction buffer (mock) before elution

from Protein G conjugated to Sepharose and subsequent binding to a slurry of peanut lectin (*Arachis hypogaea*; PNA) conjugated to beads (EY Laboratories). Material bound to lectin-beads was analyzed by SDS-PAGE and a Bio-Rad imager with Quantity One software. The data are presented as the percentage of the total construct bound to the immobilized lectin (percentage bound = (amount of construct recovered from immobilized lectin/total construct added) × 100).

Surface Staining of Polarized MDCK Cells—MDCK cells stably transfected with MUC1–22TR, 22TR-Tac, 0TR-Tac, or Tac were plated on 12-mm Costar permeable supports. Four days after plating, cells were gently rinsed on ice five times with HEPES-buffered minimum essential medium and blocked on ice in HEPES-buffered minimum essential medium containing 1% BSA for 30 min. Cells were incubated with either mouse anti-Tac (CD25, 2.5 μg/ml) or mouse anti-MUC1 TR (B27.29, 5 μg/ml) primary antibodies for 1 h on ice, washed five times, and incubated with Alexa 488-conjugated goat anti-mouse antibody (dilution 1:500; Invitrogen) for 30 min on ice. Cells were fixed on ice at room temperature in 100 mM sodium cacodylate buffer, pH 7.4, for 15 min and then permeabilized with 0.1% Triton X-100 in phosphate-buffered saline containing glycine and NH_4Cl for 5 min at room temperature. Cells were subsequently incubated with rat anti-ZO-1 hybridoma tissue culture supernatant R40.76 (gift of Gerard Apodaca (Pittsburgh, PA)) and Alexa 647-conjugated secondary antibody (Invitrogen) for 30 min at room temperature. Images were acquired using a Leica SP5-STED CW confocal microscope with a ×100 oil immersion objective (numerical aperture 1.40) equipped with argon, green helium-neon, and red helium-neon lasers in Core C of the Pittsburgh Center for Kidney Research. Images were processed with Adobe Photoshop (Adobe Systems, San Jose, CA), and single images were processed utilizing the available range of gray levels without saturation.

Knockdown of Galectin-3 (Gal-3) with siRNAs—MDCK cells with stable expression of MUC1–22TR were treated with siRNA duplexes directed to either firefly luciferase (negative control) or Gal-3 before plating cells on permeable supports as described previously (21). The polarized delivery of MUC1 and levels of Gal-3 (R&D Systems, Inc., Minneapolis, MN) and β-actin (Sigma) were assessed after 4 days by immunoblotting.

RESULTS

The Signal for Apical Targeting Is within the MUC1 Ectodomain—A prominent feature of the MUC1 ectodomain is the variable number of mucin-like TRs of 20 amino acids with five Ser/Thr residues that serve as sites for glycosylation through *O*-linked GalNAc. To assess the role of the mucin-like repeats in MUC1 apical targeting, we used metabolic labeling of MDCK cells expressing either wild-type MUC1–22TR (with 22 TRs and seven adjacent Rs), MUC1–2TR (with two TRs and seven Rs), MUC1–0R-FLAG (with a FLAG epitope tag replacing a tract containing all of the TRs, five Rs, and two *N*-glycosylation sites), and Tac-MUC1 with the ectodomain of the normally basolateral Tac (interleukin-2 receptor α subunit) replacing the entire MUC1 ectodomain (see models and sequences in Fig. 1, *A* and *B*).

Cells were starved for 30 min; pulse-labeled with [^{35}S]Met/Cys for 30 min; and chased for 30, 60, 90, and 120 min prior to biotinylation of proteins on the apical or basolateral cell surface. As expected, MUC1–22TR was efficiently delivered to the apical surface (58% of total IP was apical at 120 min), whereas only a small fraction reached the basolateral surface (maximum of 9% at 60 min) (Fig. 2), as we observed previously (10). Tac-MUC1 was delivered primarily to the basolateral surface (maximum of 26% basolateral at 60 min) with only 12% reaching the apical surface by 120 min. The data obtained for Tac-MUC1 are consistent with the loss of an apical targeting signal present within the MUC1 ectodomain and the lack of any apical targeting signal within the transmembrane or cytoplasmic domain of MUC1. Apical delivery of MUC1–2TR (48% apical at 120 min) and MUC1–0R-FLAG (25% apical at 120 min) was noticeably reduced as compared with delivery of MUC1–22TR, but basolateral delivery was not affected. Any statistically significant reductions in apical delivery and increases in basolateral delivery when compared with MUC1–22TR are indicated in Fig. 2*A* with an *asterisk*. Interestingly, apical delivery of MUC1–2TR appears delayed when compared with MUC1–22TR because apical delivery was significantly different only at the 30 and 60 min time points. Altogether, the data support the possibility that the mucin-like repeats (TR and/or R) are necessary for MUC1 delivery selectively to the apical surface of polarized MDCK cells.

The Mucin-like Repeats of MUC1 Contain the Apical Targeting Signal—We next designed experiments to determine if the mucin-like repeats of MUC1 are sufficient for apical targeting of a model protein. The N terminus of MUC1, including 22 TRs and six adjacent Rs were added to the N terminus of Tac (22TR-Tac) to determine if the mucin-like domain could reverse the polarized delivery of this model protein in a pulse-chase assay. As shown in Fig. 3, Tac was delivered primarily to the basolateral surface in polarized MDCK cells (22% of the total IP was basolateral, and 9% was apical at 120 min), whereas the chimera 22TR-Tac was delivered primarily to the apical surface (42% was apical at 120 min). Interestingly, a chimera of the six Rs attached to the N terminus of Tac (0TR-Tac) was also delivered primarily to the apical surface (29% apical at 120 min). There was a statistically significant difference in apical delivery of both 22TR-Tac and 0TR-Tac when compared with Tac at all time points ($p < 0.05$) but minimal differences in basolateral delivery of either 22TR-Tac or 0TR-Tac when compared with Tac. Although Tac was stable on the basolateral surface, levels of both 22TR-Tac and 0TR-Tac declined significantly after a 60–90-min chase. There was no statistically significant difference between 22TR-Tac and 0TR-Tac delivery to either the apical or basolateral surface.

The polarized distribution of surface ^{35}S-labeled MUC1–22TR, Tac, and chimeras observed at 120 min of chase (Figs. 2 and 3) also reflects the steady state expression of these proteins when their surface expression is analyzed by confocal immunofluorescence microscopy (Fig. 4). Although MUC1–22TR, 22TR-Tac, and 0TR-Tac exhibit primarily apical staining, Tac exhibits primarily lateral staining. At steady state, 0TR-Tac appears to have a slightly less polarized distribution compared with 22TR-Tac. This may reflect reduced stability of 0TR-Tac

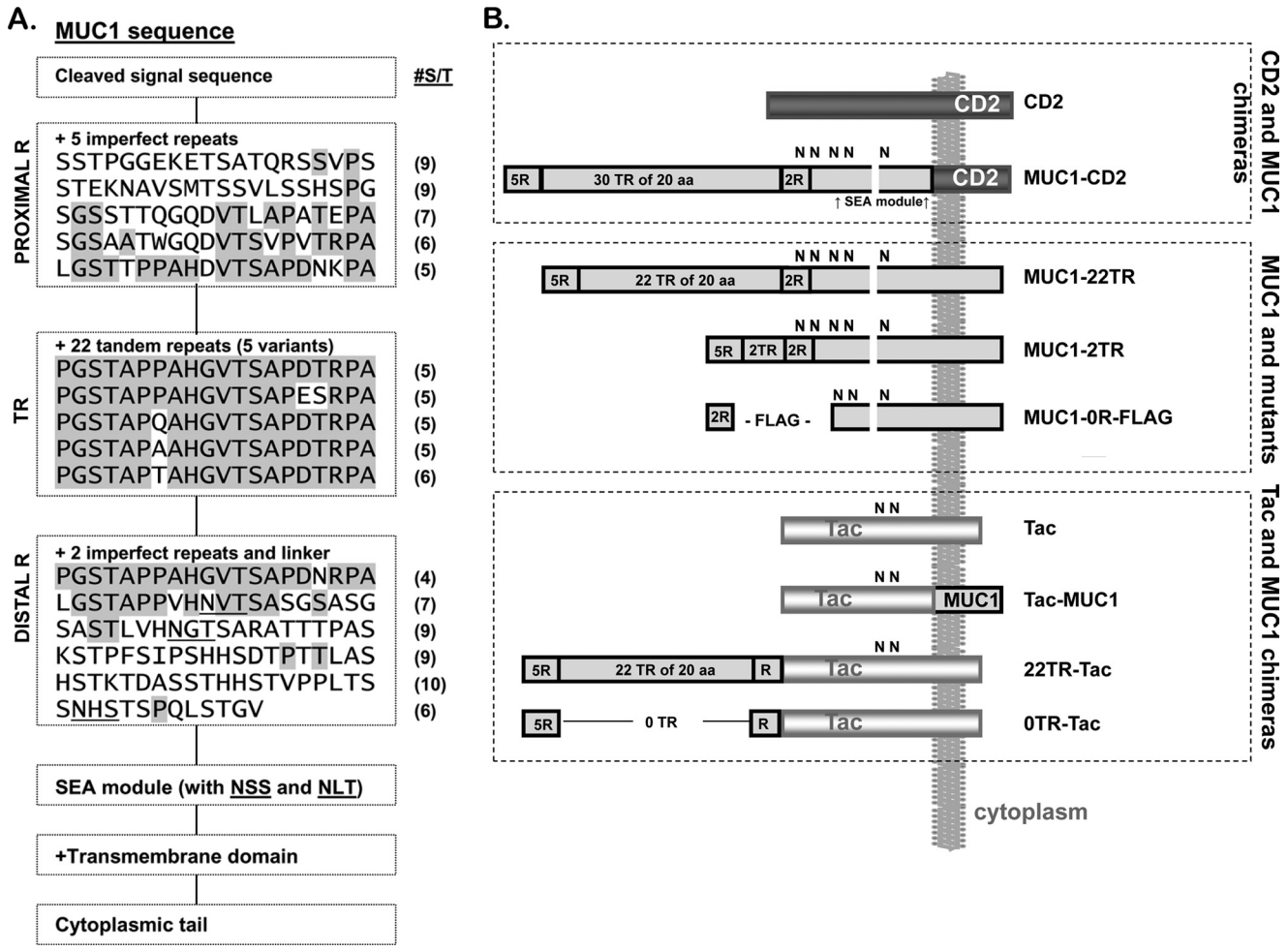

FIGURE 1. **Models of MUC1 mutants and chimeras.** MUC1 is a type 1 transmembrane protein with a cleaved signal sequence, an ectodomain including Rs and a variable number of TRs, a SEA module with autocatalytic cleavage 65 residues from the membrane, a 23-residue transmembrane domain, and a 72-residue cytoplasmic tail. *A*, amino acid sequences of the TRs and adjacent Rs are shown in *single-letter code*. There are five variants of TR, as indicated, where residues Asp-Thr are replaced by Glu-Ser or where Pro is replaced by Gln, Ala, or Thr (all have five Ser/Thr residues except the last, which has six). Conserved residues are highlighted in *gray*. There are five proximal Rs between the cleaved signal sequence and the TRs and two distal Rs between the TRs and a Ser/Thr/Pro-rich linker to the SEA module. The number of Ser/Thr residues in each R varies as indicated between four and nine. *N*-Linked glycosylation consensus sites (N*X*(S/T)) are *underlined*. *B*, schematics of constructs used in this study, including MUC1 (with 22TR or 30TR), MUC1–2TR with 2TR, MUC1-CD2 chimera, Tac-MUC1 chimera, and MUC1–0R-FLAG (with FLAG replacing a tract with all TRs, four Rs, and two *N*-glycans). MUC1 R with or without TR were appended to the N terminus of Tac to generate 0TR-Tac and 22TR-Tac, respectively.

at the apical surface, as suggested by the slightly reduced levels of 0TR-Tac apical expression observed at 120 min as compared with MUC1–22TR (Fig. 2) and 22TR-Tac (Fig. 3). Altogether, we concluded that an apical targeting signal is present within the mucin-like repeats from MUC1.

MUC1 Apical Targeting Is Not Dependent on Galectin-3—A key feature of the mucin-like domain of MUC1 is the presence of *O*-linked glycans on Ser and Thr residues (see Fig. 5*A*). Galectins (Gal) are small proteins that bind glycoconjugates containing β-galactose, such as polylactosamine, and Gal-3 is reported to play a key role in apical targeting of glycoproteins by cross-linking cargo in *trans*-Golgi network-derived vesicles (11, 12). Using a pull-down assay with the canine galectins expressed in MDCK cells (GST-tagged Gal-1, -3, -4, -7, -8, and -9) we recently found that MUC1–22TR expressed in MDCK cells binds preferentially to Gal-3 (13). Therefore, we asked if MUC1 apical targeting was Gal-3-dependent by following MUC1–22TR surface delivery in polarized MDCK cells after Gal-3 depletion by treatment of cells with siRNAs.

MDCK cells stably expressing MUC1–22TR were treated with siRNA duplexes directed to either firefly luciferase (control) or Gal-3 and plated on permeable supports as described previously (21). After 4 days in culture, we measured MUC1–22TR delivery to the apical and basolateral surface by metabolic labeling and surface biotinylation and found no difference in MUC1–22TR polarized delivery in cells treated with control or Gal-3 siRNAs, despite efficient knockdown of Gal-3 (Fig. 5*B*). Consistent with this finding, we also did not find evidence of differential levels of polylactosamine on our model proteins that exhibit primarily apical (MUC1–22TR, 22TR-Tac, and 0TR-Tac) or basolateral (Tac) delivery (Fig. 5*C*). Polarized MDCK cells expressing either MUC1–22TR, 22TR-Tac, 0TR-Tac, or Tac were metabolically labeled with [^{35}S]Met/Cys for 30 min and chased for 90 min before immunoprecipitation of the proteins. Immunoprecipitates were eluted, and equal aliquots were incubated with either WGA (control with specificity for GlcNAc or sialic acid) or LEA conjugated to beads (Fig. 5*C*). Although MUC1–22TR (68%), 22TR-Tac (63%), 0TR-Tac

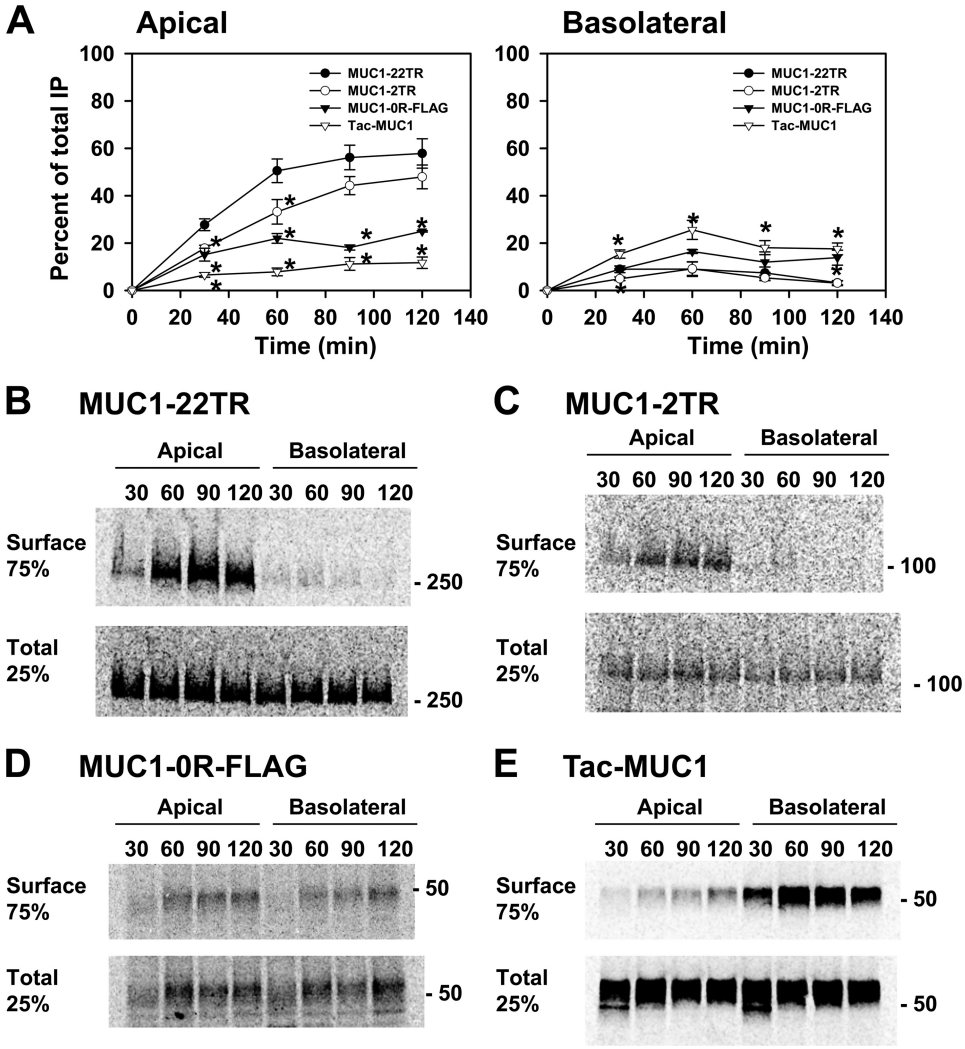

FIGURE 2. **Mucin-like repeats are necessary for MUC1 apical delivery.** Polarized MDCK cells stably expressing MUC1–22TR, MUC1–2TR, MUC1–0R-FLAG, or Tac-MUC1 were starved for 30 min, pulse-labeled for 30 min with [^{35}S]Met/Cys, and chased up to 120 min before surface biotinylation at the apical or basolateral surface. MUC1 and mutants were immunoprecipitated from cell extracts, and 25% was saved as total (*Total*), whereas 75% was incubated with avidin-conjugated beads to recover the biotinylated protein (*Surface*). Total and surface samples were analyzed after SDS-PAGE with a Bio-Rad imager. *A*, the percentage of the total MUC1 or mutant found on the cell surface is presented for multiple experiments as mean and S.E. (*error bars*) ($n = 3–6$), and statistically significant differences between the mutants and MUC1–22TR are noted by an *asterisk* (*, $p < 0.05$). Representative SDS-gel profiles are shown for MUC1–22TR (*B*), MUC1–2TR (*C*), MUC1–0R-FLAG (*D*), and Tac-MUC1 (*E*). Mobility of Bio-Rad molecular markers is indicated on the *right* of each *panel*.

(55%), and Tac (61%) all bound similarly to WGA-beads (control), we found comparable binding of MUC1–22TR (25%) and 22TR-Tac (18%) to LEA-beads but negligible binding of either 0TR-Tac (4%) or Tac (3%) (percentage bound = (amount of construct recovered from immobilized lectin/total construct added) × 100). We concluded that the presence of *O*-glycans with terminal polylactosamine on the mucin-like repeats of MUC1 does not contribute to apical targeting of MUC1.

MUC1 Imperfect Repeats Are O-Glycosylated—We next considered the possibility that shorter *O*-linked glycans could represent a key component of the apical targeting signal from MUC1. Although *O*-linked glycosylation of the TR has been well characterized on both full-length MUC1 and synthetic peptides based on MUC1 tandem repeats (22–25), glycosylation of the adjacent R has not been addressed. Within the TR, the Thr within the sequence VTSA and both the Ser and Thr within the sequence GSTA are modified, whereas the remaining two sites are used less frequently (see Fig. 1*A* and supplemental Fig. S1) (22–24). These same three predominant sites are predicted sites of glycosylation when the amino acid sequences of the TR variants are analyzed with specificity parameters developed for the polypeptide-GalNAc transferases T1, T2, T3, T5, T10, T12, and core 1 Gal transferase (26, 27). A similar analysis of the sequences of the proximal and distal imperfect R (and linker) indicates that numerous Ser and Thr are probably glycosylated such that 1–6 Ser or Thr residues are modified in each R. The results of this analysis are consistent with the presence of *O*-glycans on six R appended to Tac in both 22TR-Tac and 0TR-Tac.

To confirm that *O*-glycans are present on the six R of 0TR-Tac, we first compared binding of MUC1–22TR, 22TR-Tac, 0TR-Tac, or Tac to immobilized PNA with specificity for the non-sialylated *O*-linked core 1 glycan (Galβ1,3GalNAc-Ser/Thr) (see Fig. 5*A*). Polarized MDCK cells expressing each construct were metabolically labeled with [^{35}S]Met/Cys for 30 min and chased for 90 min before immunoprecipitation of the pro-

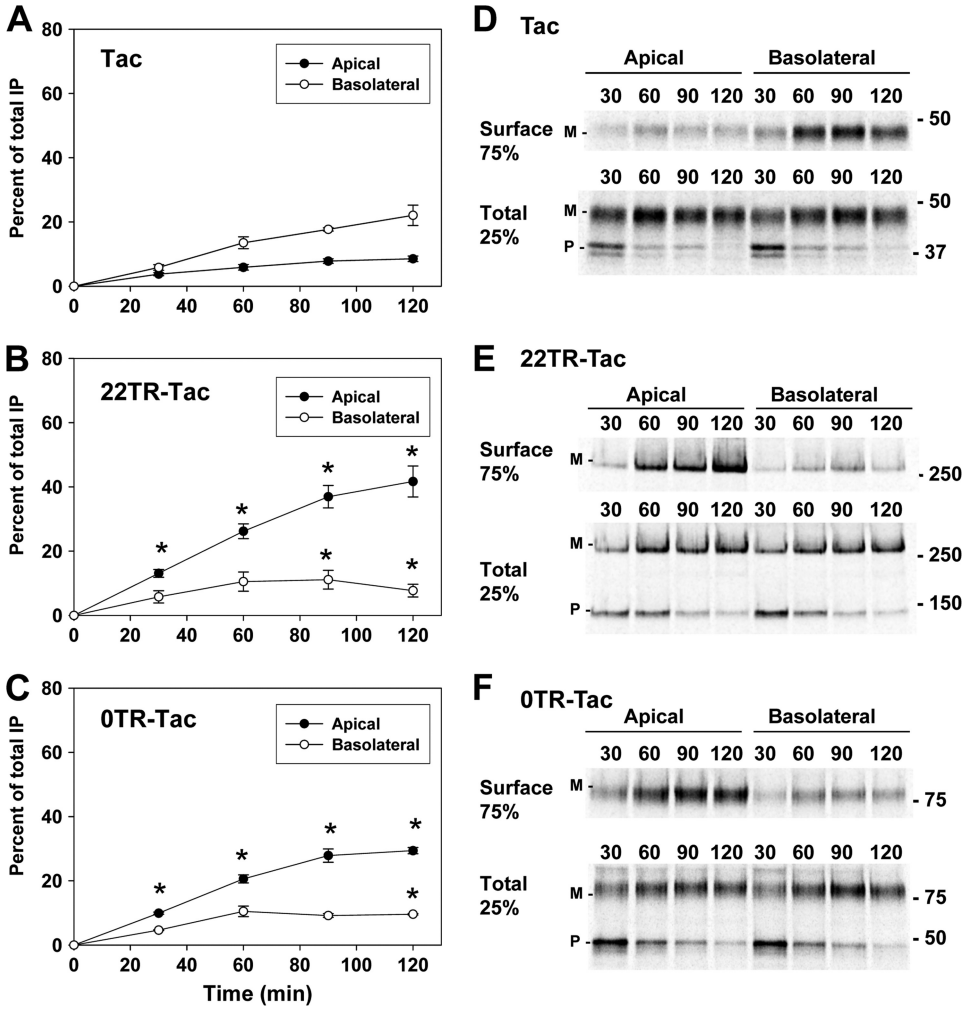

FIGURE 3. **Mucin-like repeats from MUC1 are sufficient for apical targeting of a model protein.** Polarized delivery of Tac, 22TR-Tac, or 0TR-Tac stably expressed in MDCK cells was analyzed as described in the legend to Fig. 2. The percentage of total Tac (*A*), 22TR-Tac (*B*), or 0TR-Tac (*C*) is presented for three experiments as mean and S.E. (*error bars*) Representative SDS-gel profiles (*D–F*) are shown with mature (*M*) and precursor (*P*) forms noted on the *left* and mobility of Bio-Rad molecular weight markers indicated on the *right* of each *panel*. The increase in apical delivery of 22TR-Tac and 0TR-Tac was statistically significantly different from apical delivery of Tac at all time points, whereas basolateral levels were significantly reduced when compared with Tac only at later time points (*, $p < 0.01$). There were no statistically significant differences between apical and basolateral delivery of 22TR-Tac and 0TR-Tac.

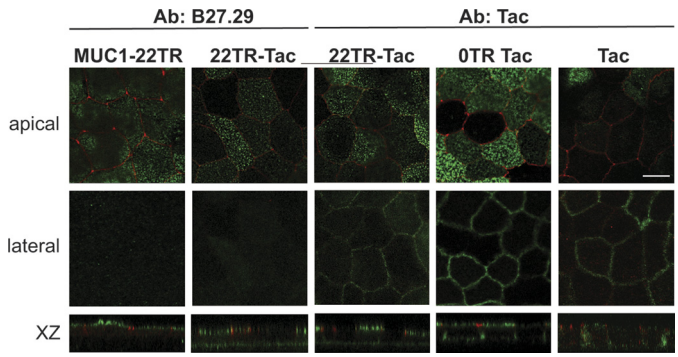

FIGURE 4. **Immunofluorescence microscopy of MUC1–22TR and chimeras in polarized MDCK cells.** Polarized MDCK cells stably expressing MUC1–22TR, Tac, or chimeras, as indicated, were blocked with 1% BSA on ice and then incubated with anti-MUC1 TR (B27.29) or anti-Tac antibodies (*Ab*) on ice to detect cell surface expression (*green*). After incubation with secondary antibodies and extensive washing, cells were fixed, permeabilized, and processed for indirect immunofluorescence to detect Z0–1 (*red*). *Single merged panels* of representative apical, lateral, and *xz* sections of each stable cell line are shown. Note that anti-Tac antibody is apparently more sensitive at detecting lateral staining of 22TR-Tac compared with B27.29. *Scale bar*, 10 μm.

teins. Immunoprecipitates were pretreated with (or without) *C. perfringens* neuraminidase for 1 h prior to elution and incubation with PNA-conjugated beads. We found appreciably greater binding of MUC1–22TR (15 and 84%), 22TR-Tac (35 and 75%), and 0TR-Tac (25 and 60%) to PNA-beads (before and after neuraminidase treatment, respectively) than Tac (2 and 19%) (Fig. 6). The levels of protein binding to PNA (MUC1–22TR, 22TR-Tac > 0TR-Tac ⋙ Tac) suggest that both the TR and the R appended to Tac are modified with core 1 *O*-glycans. We conclude that core 1 glycans are clearly present on the perfect and imperfect repeats of 22TR-Tac and 0TR-Tac and that *O*-glycans could contribute to the apical targeting of these constructs.

Core O-Glycans on Mucin-like Repeats Are a Key Feature of the Apical Targeting Signal—Because MUC1 is delivered to the apical surface by transit through the ARE, a path used by other apical proteins with glycan-dependent signals (10), and the mucin-like repeats on 0TR-Tac that direct its apical delivery are *O*-glycosylated (Fig. 6), we designed experiments to determine if *O*-glycans are a key feature of the apical targeting signal

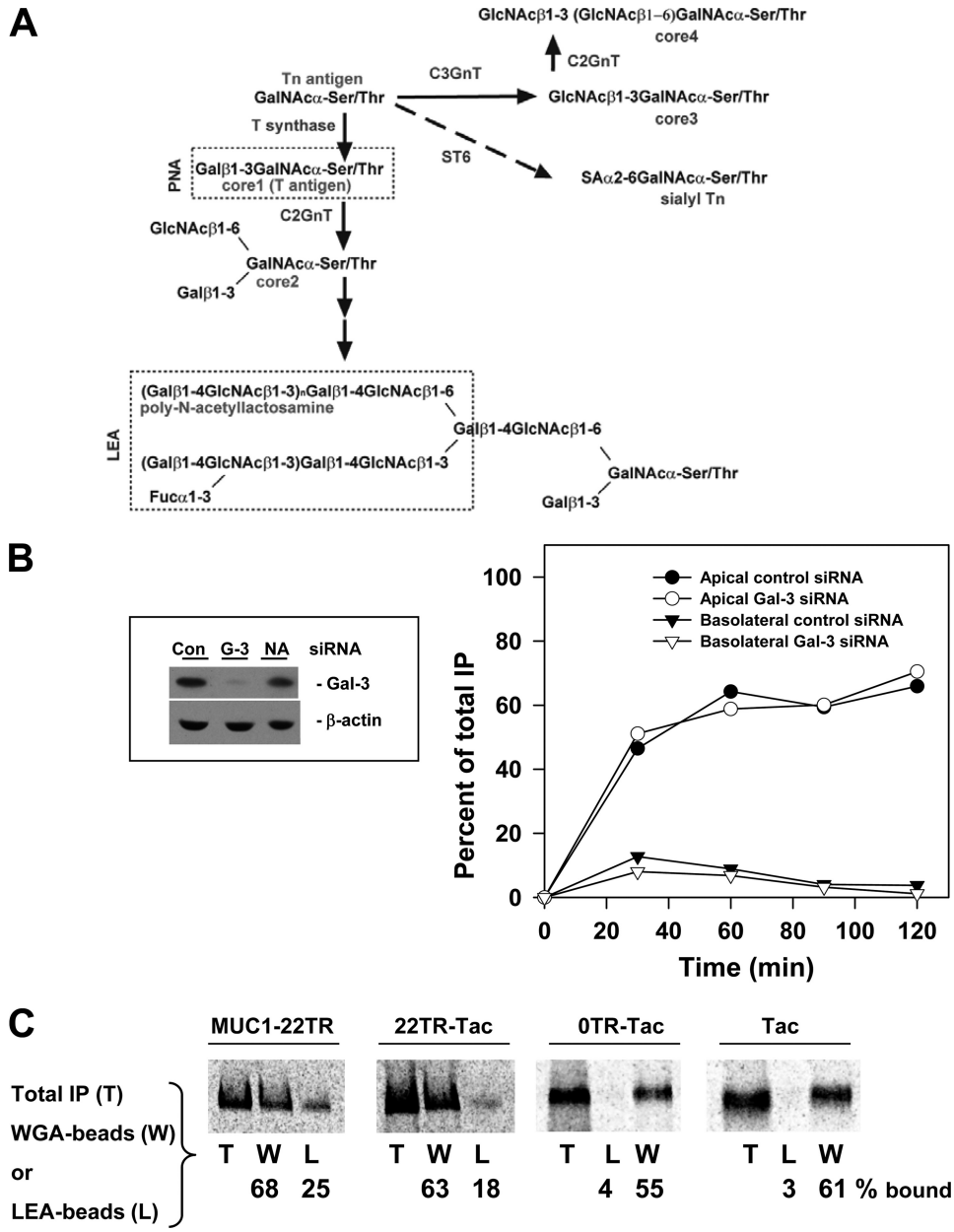

FIGURE 5. **Polarized delivery of MUC1 in MDCK cells is not Gal-3-dependent.** *A*, pathways and enzymes involved in synthesis of *O*-linked glycans. Note that PNA recognizes non-sialyated core 1, whereas LEA recognizes poly-*N*-acetyllactosamine on core 2 (see *boxed structures*). ST6GalNAc-1 (*ST6*) competes with T-synthase and core 3 synthase (*C3GnT*) for the substrate GalNAcα-Ser/Thr. *B*, MDCK cells stably expressing MUC1 were treated with siRNA duplexes directed to firefly luciferase (control) or Gal-3 and plated on permeable supports. After 4 days in culture, the polarized delivery of MUC1 was assessed by metabolic labeling for 30 min with [^{35}S]Met/Cys. After varying chase times, apical and basolateral surfaces were treated with sulfo-NHS-SS-biotin. Biotinylated MUC1 was recovered with avidin-conjugated beads from the MUC1 immunoprecipitates and analyzed with a Bio-Rad imager after SDS-PAGE. MUC1 delivery to the apical or basolateral surface is presented as the fraction of the total immunoprecipitate found on the cell surface (one representative experiment is shown, $n = 2$). Immunoblots for Gal-3 and β-actin in cell extracts after treatment with control (*Con*), Gal-3 (*G-3*), or no (*NA*) siRNAs indicate efficient depletion of Gal-3 in this experiment. *C*, polarized MDCK cells expressing MUC1–22TR, 22TR-Tac, 0TR-Tac, or Tac were metabolically labeled for 30 min with [^{35}S]Met/Cys and chased for 90 min before detergent extraction and immunoprecipitation. Immunoprecipitates were resuspended, and equal aliquots were incubated overnight with beads conjugated to WGA (*W*) or LEA (*L*) or reserved as total (*T*) before analysis after SDS-PAGE with a Bio-Rad Imager. Note that the order of total, WGA, and LEA varies between gel profiles. The *numbers below* the gel profiles indicate the percentage of total bound to each lectin (percentage bound = (amount of construct recovered from immobilized lectin/total construct added) × 100). Results from one representative experiment are shown ($n = 2$).

within the mucin-like repeats. Because there are no specific inhibitors of *O*-linked glycosylation, we stably overexpressed the enzyme ST6GalNAc-1 in MDCK cells to compete with enzymes such as core 1 Gal transferase and core 2 and core 3 GlcNAc transferases for the substrate GalNAc-Ser/Thr (see pathways in Fig. 5*A*) (18, 19, 28). Overexpression of ST6GalNAc-1 produces primarily SAα2,6GalNAc-Ser/Thr (Fig. 5, *sialyl Tn*), thereby preventing synthesis of the core *O*-glycans (*e.g.* core 1, core 2, core 3, or core 4). MDCK cells expressing ST6GalNAc-1 (MDCK+ST6) and either 0TR-Tac or Tac were pulse-labeled with [^{35}S]Met/Cys for 30 min and chased for 30, 60, 90, and 120 min prior to biotinylation of proteins on the apical or basolateral cell surface (Fig. 7). We observed that Tac was primarily delivered to the basolateral

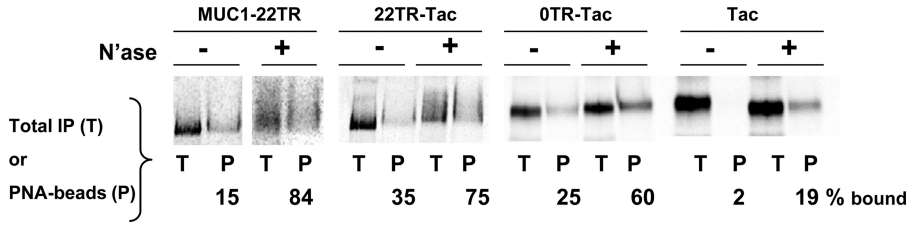

FIGURE 6. **Core 1 *O*-glycans are present on the imperfect repeats of 0TR-Tac.** Polarized MDCK cells expressing MUC1–22TR, 22TR-Tac, 0TR-Tac, or Tac were metabolically labeled for 30 min with [^{35}S]Met/Cys and chased for 90 min before detergent extraction and immunoprecipitation. Immunoprecipitates were treated (+) or mock-treated (−) with neuraminidase (*N'ase*) prior to resuspension and incubation overnight with beads conjugated to PNA (*P*) or no beads as total (*T*; note different totals for with and without neuraminidase) and analysis after SDS-PAGE with a Bio-Rad imager. The *numbers below* the gel profiles indicate the percentage of the total bound to PNA (percentage bound = (amount of construct recovered from immobilized lectin/total construct added) × 100). Results from one representative experiment are shown ($n = 2$).

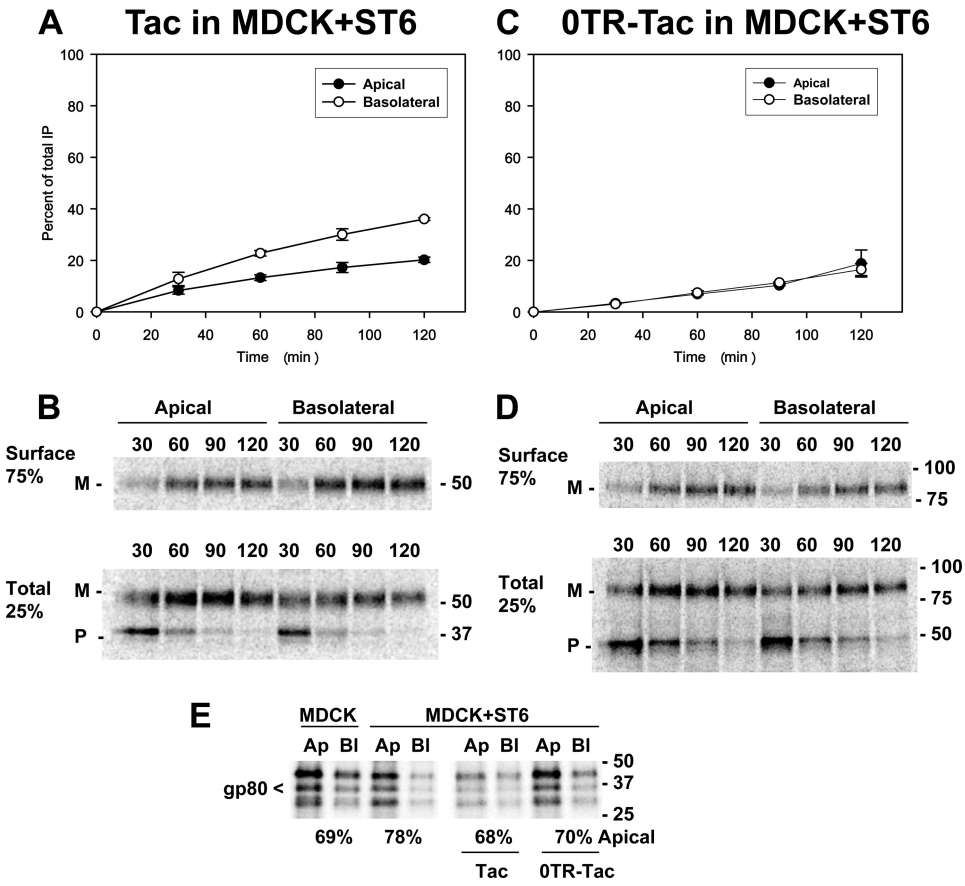

FIGURE 7. **Terminal processing of *O*-linked glycans is a key component of the MUC1 apical targeting signal.** Polarized MDCK cells stably transfected with ST6-GalNAc-1 as well as Tac or 0TR-Tac were starved for 30 min, pulse-labeled for 30 min with [^{35}S]Met/Cys, and chased up to 120 min before biotinylation at the apical or basolateral surface. Tac (*A* and *B*) and 0TR-Tac (*C* and *D*) were immunoprecipitated from cell extracts with anti-Tac antibodies, and 25% was saved as total (*Total*), whereas 75% was incubated with avidin-conjugated beads to recover the biotinylated protein (*Surface*). Total and surface samples were analyzed after SDS-PAGE with a Bio-Rad imager. *A* and *C*, the percentage of the total MUC1 or mutant found on the cell surface is presented as mean and S.E. (*error bars*) ($n = 3$). *B* and *D*, representative SDS-gel profiles are shown with mature (*M*) and precursor (*P*) forms noted on the *left* and the mobility of Bio-Rad molecular weight markers on the *right* of each *panel*. Both apical and basolateral Tac delivery had a small but significant increase in MDCK+ST6 cells when compared with MDCK cells, whereas apical 0TR-Tac delivery was significantly decreased, and basolateral 0TR-Tac delivery was increased ($p < 0.05$; compare with Fig. 3). *E*, polarized MDCK cells, MDCK+ST6 cells, or MDCK+ST6 cells expressing Tac or 0TR-Tac were starved for 30 min, pulse-labeled for 30 min with [^{35}S]Met/Cys, and chased for 120 min. Aliquots from the apical and basolateral medium were analyzed after SDS-PAGE with a Bio-Rad imager. The three radiolabeled bands between 30 and 50 kDa representing cleaved gp80 were quantified. The *numbers below* the gel are the percentage of the total gp80 (apical + basolateral) found in the apical medium. A representative gel profile is presented ($n = 2$).

surface of MDCK+ST6 cells (36% basolateral and 20% apical at 120 min of chase), similar to its delivery in wild-type MDCK cells (Fig. 3*A*). However, 0TR-Tac delivery to the surface of MDCK+ST6 cells was non-polarized (19% apical and 16% basolateral at 120 min), which was very different from its primarily apical delivery in wild-type MDCK cells (Fig. 3*C*).

To ensure that MDCK+ST6 cells expressing 0TR-Tac were still capable of apical targeting, we assessed secretion of the endogenous protein gp80. The apical targeting of gp80 is dependent on the presence of *N*-linked glycans (29). Both MDCK+ST6 cells (non-transfected or stably transfected with either 0TR-Tac or Tac) and control MDCK cells were pulse-labeled with [^{35}S]Met/Cys for 30 min and chased for 120 min before recovery of the culture medium. In every case, [^{35}S]gp 80 was secreted primarily into the apical medium (68–78%), indicating that overexpression of ST6GalNAc-1 does not disrupt

the polarity of MDCK cells (Fig. 7*E*). We concluded that core *O*-linked glycosylated mucin-like repeats of MUC1 can function as an apical targeting signal.

DISCUSSION

In this study, we observed that (i) deletion of the mucin-like repeats from MUC1 reduced apical delivery without affecting basolateral delivery, (ii) adding the mucin-like repeats of MUC1 to Tac enhanced its apical delivery without affecting basolateral delivery, and (iii) overexpression of ST6GalNAc-1 blocked the apical targeting activity of the mucin-like repeats. The cumulative data indicate that core-glycosylated mucin-like repeats within MUC1 represent an apical targeting signal.

N-Linked Glycans Are Not Required for MUC1 Apical Targeting—Pemberton *et al.* (15) previously concluded that apical targeting information was found within the MUC1 ectodomain by characterizing chimeras of MUC1 and CD2 in MDCK cells. Concurrently, the results of our studies with chimeras of MUC1 and Tac also indicated that an apical targeting signal was present within the MUC1 ectodomain. We also suspected that the apical targeting signal would be glycan-dependent because a dominant feature of MUC1 is its heavily glycosylated mucin-like domain. Also, we had already found that MUC1 transits the apical recycling endosome, a path used by other apically destined proteins with glycan-dependent targeting signals, such as the sialomucin endolyn (10). Although endolyn exhibits both *N*-linked and *O*-linked glycans, Potter *et al.* (30) found that its apical targeting was fully dependent on terminal processing of two specific *N*-glycans. However, in preliminary experiments, we found that treatment of cells with kifunensine to block terminal processing of *N*-glycans had no effect on MUC1 apical delivery.[4] Our subsequent analysis of MUC1 mutants lacking all five consensus sites for *N*-glycosylation was impaired by its consistently low level of expression, but immunoblot analysis of polarized MDCK cells revealed that the mutant was still expressed primarily on the apical surface.[5] Overall, these data led us to focus on the role of *O*-linked glycosylation in MUC1 apical targeting.

MUC1 Apical Targeting Is Not Galectin-3-dependent—The primary feature of the MUC1 mucin-like domain is the presence of Ser/Thr/Pro-rich nearly perfect tandem repeats that exhibit at least three sites for *O*-glycosylation in each repeat. Because we found that mutations that removed most (2TR-MUC1) or all of the tandem repeats (MUC1–0R-FLAG) correspondingly reduced apical delivery, the data were consistent with the presence of synergistic apical targeting signals within the tandem repeats. However, the deletion within the MUC1–0R-FLAG mutant also removed imperfect repeats, which fits with our subsequent discovery that targeting information was present with these latter tracts. We were surprised to find that apical targeting information was present within the imperfect repeats of MUC1 because it was not known whether these sequences were actually modified with *O*-linked glycans. Although analysis of the amino acid sequence of these imperfect repeats with specificity parameters developed for several of the polypeptide-GalNAc transferases predicted numerous sites for *O*-linked glycosylation, we subsequently found that Tac binding to immobilized peanut lectin with specificity for core 1 *O*-glycans was notably enhanced by the addition of the imperfect repeats to the N terminus of Tac (0TR-Tac). However, attachment of the imperfect repeats to Tac did not enhance its binding to immobilized tomato lectin with specificity for polylactosamine that represents terminal processing of core 2 glycans, indicating that core glycosylation rather than polylactosamine was more likely a key feature of the apical targeting signal.

The lack of polylactosamine on the apical 0TR-Tac was also consistent with our finding that Gal-3 plays no role in apical targeting of MUC1–22TR. Several facts were consistent with the possibility that Gal-3 might play a role in MUC1 apical targeting: (i) Gal-3 has been implicated in apical targeting in MDCK cells of the glycoprotein phlorizin lactate hydrolase with glycan-dependent targeting (31); (ii) Gal-3 is the most abundant galectin in MDCK cells and exhibits a preference for polylactosamine on both *N*-linked and *O*-linked glycans with either terminal blood group A, sialic acid (α2,6), or fucose (13, 32); and (iii) MUC1–22TR synthesized in MDCK cells exhibits polylactosamine and binds preferentially to Gal-3 in pull-down assays with all of the endogenous canine galectins (13). However, we consistently observed that efficient depletion of Gal-3 in MDCK cells using treatment with siRNAs had no effect on MUC1 apical delivery.

Core O-Glycans Are a Key Feature of the MUC1 Apical Targeting Signal—Because the polylactosamine found on MUC1–22TR and 22TR-Tac was seemingly irrelevant to MUC1 apical targeting, we focused our analysis on the presence of core glycans by overexpression of ST6GalNAc-1 to terminate *O*-glycans at SAα2,6GalNAc-Ser/Thr. The absence of core glycans on 0TR-Tac in MDCK+ST6 cells did block its apical delivery, whereas Tac polarized delivery in MDCK+ST6 cells was unchanged, indicating that core glycans (*e.g.* core 1, 2, 3, or 4) on the imperfect (and maybe nearly perfect) repeats represented the apical targeting signal for MUC1. We did test this conclusion by analyzing MUC1–22TR synthesis in cells overexpressing ST6GalNAc-1, but we did not observe a reduction in apical delivery.[4] Because we found that MUC1–22TR binding to LEA-conjugated beads was reduced only 70% in MDCK+ST6 cells as compared with MUC1–22TR expressed in wild-type MDCK cells, we suspect that the level of ST6GalNAc-1 expression was not sufficient to block terminal processing of enough *O*-glycan sites in MUC1–22TR (66 sites in 22 TRs plus 18 sites in seven Rs). However, this level of ST6GalNAc-1 overexpression was adequate to block terminal processing of the relevant *O*-glycan sites in 0TR-Tac (16 sites in six Rs) (see supplemental Fig. S1 for prediction of Ser and Thr modified by *O*-glycosylation).

Mechanism of Glycan-dependent Apical Trafficking—*O*-Glycans on apical glycoproteins have been implicated previously (33, 34) as a key feature of the apical targeting signal of the neurotrophin receptor p75 and sucrase-isomaltase. More recently, Lee *et al.* (35) reported that terminal processing of *O*-glycans by specifically core 2 GlcNAc transferase-2 is essential for surface expression of the apical sucrase-isomaltase and dipeptidylpeptidase IV in intestinal epithelial cells (35). They found that cell surface levels of sucrase-isomaltase and dipeptidyl-

[4] C. L. Kinlough and R. P. Hughey, unpublished data.
[5] S. J. Gendler, C. L. Kinough, and R. P. Hughey, unpublished data.

peptidase IV are greatly reduced in Caco-2 intestinal epithelial cells after core 2 GlcNAc transferase-2 knockdown with RNAi or after overexpression of core 3 synthase that blocks synthesis of core 2 structures in HT-29 intestinal epithelial cells (35). The requirement for core 2 *O*-glycans for any surface expression of dipeptidylpeptidase IV is probably the basis for the earlier reports showing that treatment of HT-29 intestinal cells with benzyl-GalNAc blocked dipeptidylpeptidase IV and MUC1 steady state cell surface expression (36, 37). Interestingly, we did not find any change in MUC1 apical delivery in MDCK cells after metabolic labeling in the presence of the related compound phenyl-GalNAc,[4] suggesting either that these inhibitors have differential effects in intestinal and renal epithelial cells or that apical targeting pathways differ in these two types of epithelia.

A key question that remains unanswered is how and where glycans enable apical sorting. One hypothesis is that glycans play purely a structural role in maintaining transport-competent conformation of apically destined proteins. Alternatively, glycan-dependent sorting receptors, possibly galectins, have been suggested to facilitate sorting (9, 38, 39). Segregation of apically and basolaterally destined proteins first occurs in the *trans*-Golgi network, although many proteins subsequently traverse endocytic compartments prior to reaching the cell surface (40, 41). Apical proteins that associate with glycolipid-enriched rafts apparently traffic through apical early endosomes, whereas non-raft-associated proteins may enter the ARE prior to surface delivery (31, 42, 43). The observation that proteins with glycan-dependent apical sorting signals, including endolyn, p75, and now MUC1, transit the ARE suggests that segregation of glycan-dependent proteins occurs by a common mechanism along this pathway (10, 44). Whether selection involves default routing to the ARE or active sorting at an earlier step remains to be determined.

Acknowledgments—We thank Franz Hanisch and Henrik Clausen for helpful discussions and Tom Gerken for analysis of the MUC1 sequence with specificity parameters developed for the polypeptide-GalNAc transferases.

REFERENCES

1. Hattrup, C. L., and Gendler, S. J. (2008) *Annu. Rev. Physiol.* **70,** 431–457
2. Kufe, D. W. (2009) *Nat. Rev. Cancer.* **9,** 874–885
3. Rahn, J. J., Dabbagh, L., Pasdar, M., and Hugh, J. C. (2001) *Cancer* **91,** 1973–1982
4. McGuckin, M. A., Walsh, M. D., Hohn, B. G., Ward, B. G., and Wright, R. G. (1995) *Hum. Pathol.* **26,** 432–439
5. Kinlough, C. L., Poland, P. A., Bruns, J. B., Harkleroad, K. L., and Hughey, R. P. (2004) *J. Biol. Chem.* **279,** 53071–53077
6. Kinlough, C. L., McMahan, R. J., Poland, P. A., Bruns, J. B., Harkleroad, K. L., Stremple, R. J., Kashlan, O. B., Weixel, K. M., Weisz, O. A., and Hughey, R. P. (2006) *J. Biol. Chem.* **281,** 12112–12122
7. Altschuler, Y., Kinlough, C. L., Poland, P. A., Bruns, J. B., Apodaca, G., Weisz, O. A., and Hughey, R. P. (2000) *Mol. Biol. Cell* **11,** 819–831
8. Potter, B. A., Hughey, R. P., and Weisz, O. A. (2006) *Am. J. Physiol. Cell Physiol.* **290,** C1–C10
9. Weisz, O. A., and Rodriguez-Boulan, E. (2009) *J. Cell Sci.* **122,** 4253–4266
10. Mattila, P. E., Kinlough, C. L., Bruns, J. R., Weisz, O. A., and Hughey, R. P. (2009) *Biol. Chem.* **390,** 551–556
11. Delacour, D., Cramm-Behrens, C. I., Drobecq, H., Le Bivic, A., Naim, H. Y., and Jacob, R. (2006) *Curr. Biol.* **16,** 408–414
12. Delacour, D., Greb, C., Koch, A., Salomonsson, E., Leffler, H., Le Bivic, A., and Jacob, R. (2007) *Traffic* **8,** 379–388
13. Poland, P. A., Rondanino, C., Kinlough, C. L., Heimburg-Molinaro, J., Arthur, C. M., Stowell, S. R., Smith, D. F., and Hughey, R. P. (2011) *J. Biol. Chem.* **286,** 6780–6790
14. Ten Hagen, K. G., Fritz, T. A., and Tabak, L. A. (2003) *Glycobiology* **13,** 1R–16R
15. Pemberton, L. F., Rughetti, A., Taylor-Papadimitriou, J., and Gendler, S. J. (1996) *J. Biol. Chem.* **271,** 2332–2340
16. Poland, P. A., Kinlough, C. L., Rokaw, M. D., Magarian-Blander, J., Finn, O. J., and Hughey, R. P. (1997) *Glycoconj. J.* **14,** 89–96
17. Kohlgraf, K. G., Gawron, A. J., Higashi, M., Meza, J. L., Burdick, M. D., Kitajima, S., Kelly, D. L., Caffrey, T. C., and Hollingsworth, M. A. (2003) *Cancer Res.* **63,** 5011–5020
18. Sewell, R., Bäckström, M., Dalziel, M., Gschmeissner, S., Karlsson, H., Noll, T., Gätgens, J., Clausen, H., Hansson, G. C., Burchell, J., and Taylor-Papadimitriou, J. (2006) *J. Biol. Chem.* **281,** 3586–3594
19. Marcos, N. T., Bennett, E. P., Gomes, J., Magalhaes, A., Gomes, C., David, L., Dar, I., Jeanneau, C., Defrees, S., Krustrup, D., Vogel, L. K., Kure, E. H., Burchell, J., Taylor-Papadimitriou, J., Clausen, H., Mandel, U., and Reis, C. A. (2011) *Front. Biosci.* **3,** 1443–1455
20. Schroeder, J. A., Thompson, M. C., Gardner, M. M., and Gendler, S. J. (2001) *J. Biol. Chem.* **276,** 13057–13064
21. Mo, D., Potter, B. A., Bertrand, C. A., Hildebrand, J. D., Bruns, J. R., and Weisz, O. A. (2010) *Am. J. Physiol. Renal Physiol.* **299,** F1178–F1184
22. Wandall, H. H., Hassan, H., Mirgorodskaya, E., Kristensen, A. K., Roepstorff, P., Bennett, E. P., Nielsen, P. A., Hollingsworth, M. A., Burchell, J., Taylor-Papadimitriou, J., and Clausen, H. (1997) *J. Biol. Chem.* **272,** 23503–23514
23. Müller, S., Goletz, S., Packer, N., Gooley, A., Lawson, A. M., and Hanisch, F. G. (1997) *J. Biol. Chem.* **272,** 24780–24793
24. Müller, S., Alving, K., Peter-Katalinic, J., Zachara, N., Gooley, A. A., and Hanisch, F. G. (1999) *J. Biol. Chem.* **274,** 18165–18172
25. Hanisch, F. G., and Müller, S. (2000) *Glycobiology* **10,** 439–449
26. Gerken, T. A., Raman, J., Fritz, T. A., and Jamison, O. (2006) *J. Biol. Chem.* **281,** 32403–32416
27. Miwa, H. E., Gerken, T. A., Jamison, O., and Tabak, L. A. (2010) *J. Biol. Chem.* **285,** 1208–1219
28. Brockhausen, I. (1999) *Biochim. Biophys. Acta* **1473,** 67–95
29. Parczyk, K., and Koch-Brandt, C. (1991) *FEBS Lett.* **278,** 267–270
30. Potter, B. A., Ihrke, G., Bruns, J. R., Weixel, K. M., and Weisz, O. A. (2004) *Mol. Biol. Cell* **15,** 1407–1416
31. Jacob, R., and Naim, H. Y. (2001) *Curr. Biol.* **11,** 1444–1450
32. Friedrichs, J., Torkko, J. M., Helenius, J., Teräväinen, T. P., Füllekrug, J., Muller, D. J., Simons, K., and Manninen, A. (2007) *J. Biol. Chem.* **282,** 29375–29383
33. Yeaman, C., Le Gall, A. H., Baldwin, A. N., Monlauzeur, L., Le Bivic, A., and Rodriguez-Boulan, E. (1997) *J. Cell Biol.* **139,** 929–940
34. Jacob, R., Alfalah, M., Grünberg, J., Obendorf, M., and Naim, H. Y. (2000) *J. Biol. Chem.* **275,** 6566–6572
35. Lee, S. H., Yu, S. Y., Nakayama, J., Khoo, K. H., Stone, E. L., Fukuda, M. N., Marth, J. D., and Fukuda, M. (2010) *J. Biol. Chem.* **285,** 37683–37692
36. Huet, G., Hennebicq-Reig, S., de Bolos, C., Ulloa, F., Lesuffleur, T., Barbat, A., Carrière, V., Kim, I., Real, F. X., Delannoy, P., and Zweibaum, A. (1998) *J. Cell Biol.* **141,** 1311–1322
37. Delacour, D., Gouyer, V., Leteurtre, E., Ait-Slimane, T., Drobecq, H., Lenoir, C., Moreau-Hannedouche, O., Trugnan, G., and Huet, G. (2003) *J. Biol. Chem.* **278,** 37799–37809
38. Rodriguez-Boulan, E., and Gonzalez, A. (1999) *Trends Cell Biol.* **9,** 291–294
39. Delacour, D., Koch, A., and Jacob, R. (2009) *Traffic* **10,** 1405–1413
40. Cramm-Behrens, C. I., Dienst, M., and Jacob, R. (2008) *Traffic* **9,** 2206–2220
41. Fölsch, H., Mattila, P. E., and Weisz, O. A. (2009) *Traffic* **10,** 972–981
42. Polishchuk, R., Di Pentima, A., and Lippincott-Schwartz, J. (2004) *Nat. Cell Biol.* **6,** 297–307
43. Guerriero, C. J., Lai, Y., and Weisz, O. A. (2008) *J. Biol. Chem.* **283,** 18040–18047
44. Cresawn, K. O., Potter, B. A., Oztan, A., Guerriero, C. J., Ihrke, G., Goldenring, J. R., Apodaca, G., and Weisz, O. A. (2007) *EMBO J.* **26,** 3737–3748